



Mapping the mantle lithosphere for diamond potential using teleseismic methods[☆]

D.B. Snyder^{a,*}, S. Rondenay^b, M.G. Bostock^c, G.D. Lockhart^d

^a*Geological Survey of Canada, 615 Booth Street, Ottawa, ON, Canada K1A 0E9*

^b*Department of Earth and Planetary Sciences, MIT, Cambridge, MA, USA*

^c*Department of Earth and Ocean Sciences, University of British Columbia, Vancouver, BC, Canada V6T1Z1*

^d*BHP-Billiton Diamonds Inc., Kelowna, BC, Canada V1X 4L1*

Received 27 June 2003; accepted 9 January 2004

Available online 20 July 2004

Abstract

Recent developments in seismic, magnetotelluric and geochemical analytical techniques have significantly increased our capacity to explore the mantle lithosphere to depths of several hundred kilometres, to map its structures, and through geological interpretations, to assess its potential as a diamond reservoir. Several independent teleseismic techniques provide a synergistic approach in which one technique compensates for inadequacies in another. Shear wave anisotropy and discontinuity studies using single seismic stations define vertical mantle stratigraphic columns. For example, beneath the central Slave craton seismic discontinuities at depths of 38, 110, 140 and 190 km appear to bound two distinct anisotropic layers. Tomographic (3-D) inversions of seismic wave travel-times and 2-D inversions of surface or scattered waves use arrays of stations and provide lateral coverage. In combination, and by correlation with electrical conductivity and xenolith petrology studies, these techniques provide maps of key physical properties within parts of the cratons known to host diamonds. Beneath the Slave craton, the discontinuity at 38 km is the base of the crust; the boundaries at 110 and 140 km appear to bound a layer of depleted harzburgite that is interpreted to contain graphite. To date, only some of these techniques have been applied to the Slave and Kaapvaal cratons so that the origin and geological history of the currently mapped mantle structures are not, as yet, generally agreed.

© 2004 Elsevier B.V. All rights reserved.

Keywords: Slave craton; Diamond exploration; Seismic imaging; Lithospheric discontinuity; Craton stabilization

1. Introduction

Diamond deposits are typically identified in four stages: (1) regional targeting, during which a region's

potential is assessed, often by mapping of Archean age basement, grid sampling for indicator minerals or global seismological mapping of continental mantle 'keels'; (2) kimberlite detection, during which glacial till mapping and high-resolution aeromagnetic surveys locate individual kimberlite deposits; (3) deposit delineation, in which drill hole core sampling determines a specific deposit's volume and lithology; and (4) evaluation, in which bulk sampling establishes a

[☆] Supplementary data associated with this article can be found, in the online version, at doi: 10.1016/j.lithos.2004.03.049.

* Corresponding author. Tel.: +1-613-992-9240; fax: +1-613-943-9285.

E-mail address: dsnyder@nrcan.gc.ca (D.B. Snyder).

deposit's worth and its feasibility to be mined. The diamond exploration industry needs discriminating tools to reduce risks at all of these four stages.

Very approximate statistics from the past few decades indicate that globally, for every 1000 candidate magnetic anomalies identified, 100 are kimberlites, 10 contain gem-quality diamonds and 1 is economic to mine in remote areas. The central part of the Slave craton appears to be more prospective than the remainder, and seismic imaging is helpful in discerning which parts are more likely to host economic deposits. More specifically, at the Ekati Diamond Mine™, 150 kimberlites have been discovered at an 80% success rate and approximately 1 pipe in 15 may be economic. In other parts of the Slave, the Dry Bones Bay area or the Coronation Gulf area, for example, it appears improbable that a commercial property will be found. Seismic techniques can provide three-dimensional (3-D) maps of key physical properties in the mantle to 700 km depth to help accomplish stage one (Nolet et al., 1994; Bostock, 1999). These results can then be used to interpret mantle structure in conjunction with conductivity maps derived from magnetotelluric soundings and the 'ground truth' of actual rock types provided by rare xenolith samples from kimberlites. If such multi-disciplinary upper mantle studies were performed on other cratonic terrains, it may be possible to prioritize where exploration should be focused.

At present, our efforts at refining suitable seismological techniques are concentrated in the central Slave craton of the NW Territories, Canada (Fig. 1), because of the strong geological, geophysical and logistical base currently available. Once a velocity and physical property model is established in the Slave craton with sufficient detail with which to help assess diamond occurrences, this innovative, first-order adaptation of seismic exploration tools can be applied throughout Canada and globally. Here, we describe our progress to date in adapting a number of established and newly developed seismological analysis tools to this special exploration application.

2. Equipment and classification of teleseismic methods

Seismic methods applied to the delineation of Earth structure fall into two broad categories: (1) 3-D map-

ping of seismic wave transmission via travel-times and (2) studies of forward- or back-scattered wave fields. Logistically, these methods divide into different groupings: those using single, independent stations recording many distant (teleseismic) earthquakes and those using an array of stations that all record the same seismic wave source, be it teleseismic or man-made. Each method provides a different feature or characteristic of the Earth model, for example: bulk compressional wave (P-wave) or shear wave (S-wave) velocities, depths and geometries of discontinuities, direction of fabric or anisotropy. In remote, harsh environments such as the central Slave craton, it is prudent to begin with single station studies, assess the results and then develop arrays of stations in key areas. Two methods that utilize a single station are currently being applied in the Slave and their results are assessed herein. A low-resolution, regional-scale array study has also begun.

Seismograms from four years of recording global earthquakes using a few broadband seismometers located near the Ekati Diamond Mine™ can be analyzed by the independent SKS-anisotropy and receiver-function techniques to reveal information about layered structure within the upper mantle of the central Slave craton. Within the past two years, 22 POLARIS satellite-telemetry stations (www.polarisnet.ca) have supplemented recent fieldwork that used a few stations with interchangeable hard-disc recorders (Snyder et al., 2002) and a more regional survey done in 1996–1998 (Bank et al., 2000) (Fig. 1; online Appendix A).

Each POLARIS telemetry station costs about C\$60,000 to purchase, transport and install at a remote location in Canada's North. A typical station consists of a GURALP 3ESP sensor with a nominal bandwidth of 0.033 to 50 Hz, a Nanometrics Libra digitizer, satellite uplink electronics, and 16 12-V batteries charged by a 12-panel solar power subsystem. The earlier stations used GURALP 40 T seismometers (0.05 to 50 Hz bandwidth), Nanometrics Orion portable recorders, and similar but smaller power subsystems (Snyder et al., 2002).

3. Discontinuity detection

The first method applied to data from independent, single stations is the so-called receiver function method in which source-deconvolved P-to-S converted

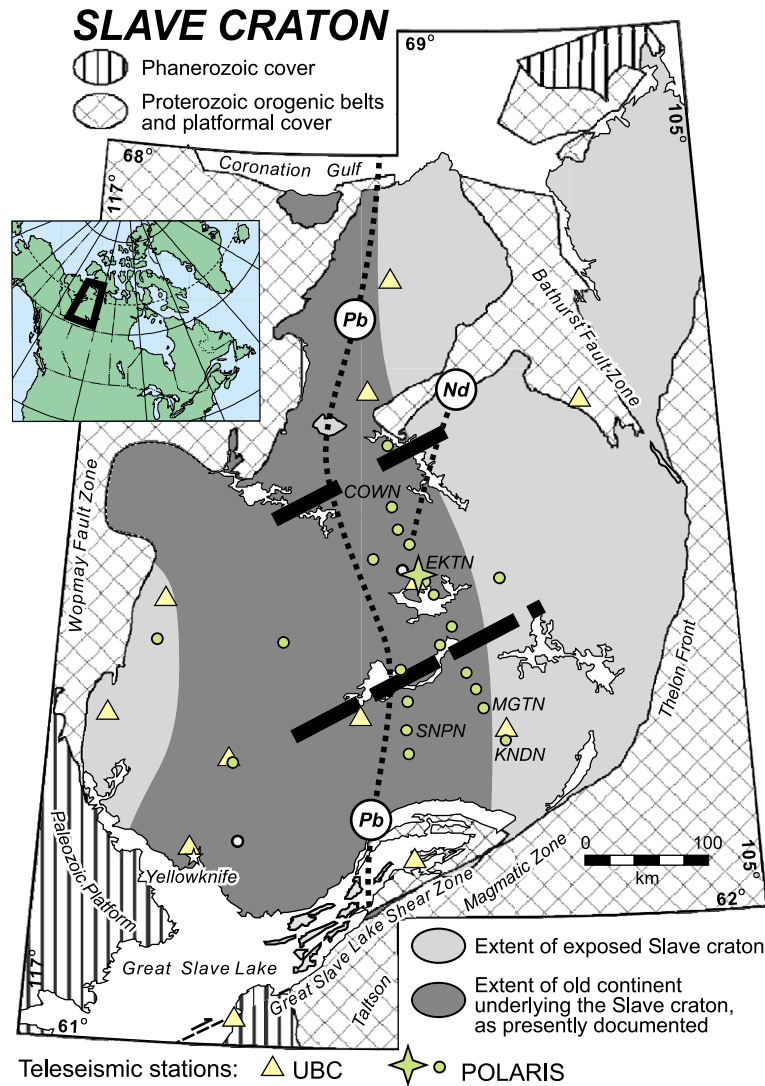


Fig. 1. Location map of the POLARIS and earlier teleseismic arrays in the central Slave craton, Northwest Territories (NWT), Canada. The heavy dashed lines indicate zoning within the mantle as described by Grütter et al. (1999); crustal isotopic zonation is described by Davis et al. (1996).

waves arriving from multiple teleseismic earthquakes reveal discontinuities in seismic wave velocities or density below each seismic station (Fig. 2) (Bostock, 1998, 1999). These discontinuities represent local increases in the rate at which physical properties vary with increasing depth. Changes in velocity, density or anisotropy within the mantle over a depth range that is a fraction of the seismic wavelength scatter upcoming seismic waves and partially convert P-waves into S-

waves to reveal the discontinuities. Typically, the sharp (to seismic waves with wavelengths of a few kilometers) increase in both velocity and density with depth at the Moho (roughly the base of the crust) is the most prominent and laterally extensive of these discontinuities (Figs. 3 and 4). Within the central Slave craton, Moho depth determined by this method varies between 36 and 42 km (Fig. 3). At the Ekati Diamond Mine™ station (EKTN), the Moho shows

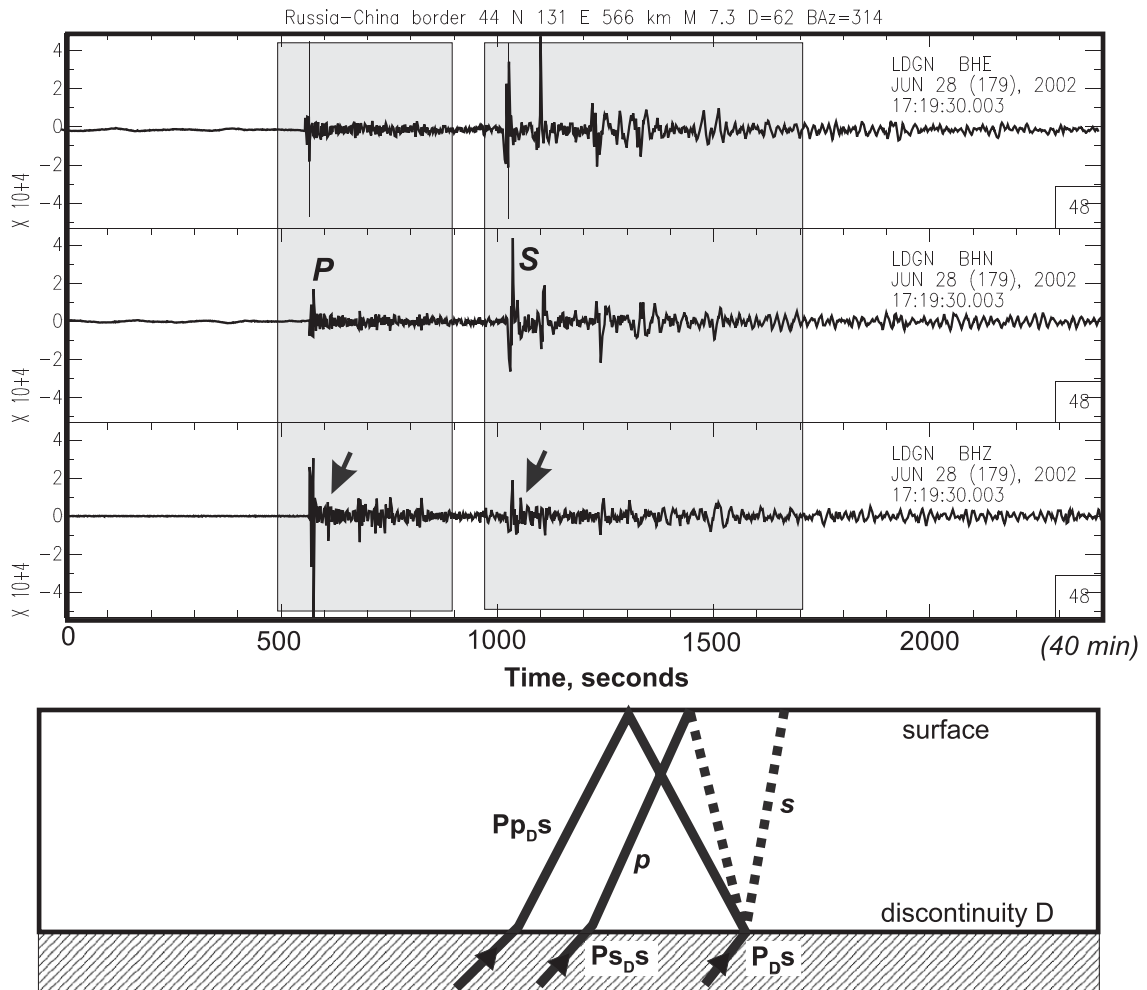


Fig. 2. (Top) Example of an earthquake recorded by the POLARIS NWT array. Here, an earthquake 566 km below the Russia–China border as recorded 62° (7000 km) away at the Lac de Gras station (LDGN). Windows indicate impulsive P-wave and S-wave arrivals and later arrivals from conversions at discontinuities (arrows). (Bottom) Schematic of possible conversions at one discontinuity that cause later arrivals.

little variation with changing direction of arrival (back azimuth) of the seismic wave (Fig. 4a); here, that statement applies within an annular ring (a ‘doughnut’) between radii of 6 and 12 km. At 130 km depth, a similar ring of illumination has radii of 23 and 48 km because each station senses physical properties within a cone beneath it.

Reverberations or ‘multiples’ of energy between the surface and strong discontinuities such as the Moho are relatively well understood and can be easily recognized by their polarity and move-out response (changes in travel time with increased offset between

earthquake source and receiver, see Bostock, 1998). These reverberations can often have correlation amplitudes similar to the primary converted S-wave (Figs. 3 and 4a). Within the Slave craton, the Moho discontinuity generally shows no response on the transverse components and therefore no Moho ‘multiples’ should appear on these components. Our analysis therefore focuses on prominent and consistent discontinuities with polarities different than predicted Moho ‘multiples’ that manifest themselves on either the transverse or radial components (e.g. 107 km discontinuity beneath EKTN, Figs. 3 and 4).

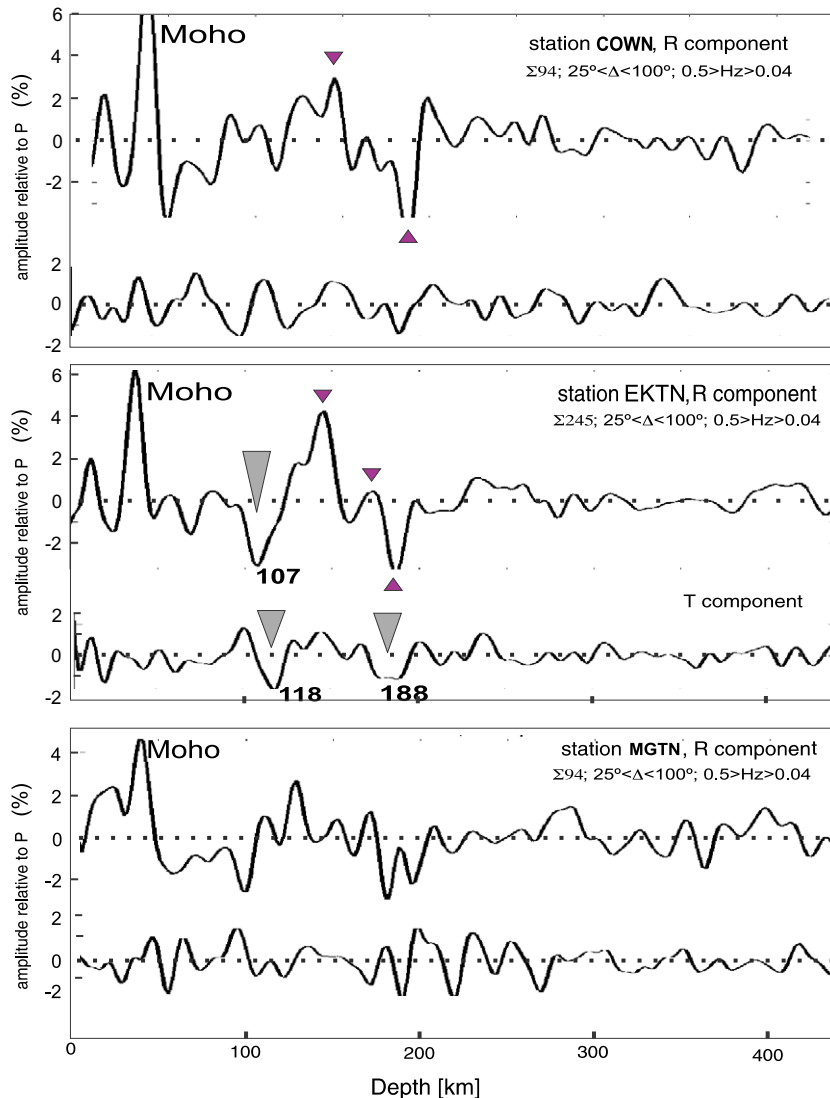


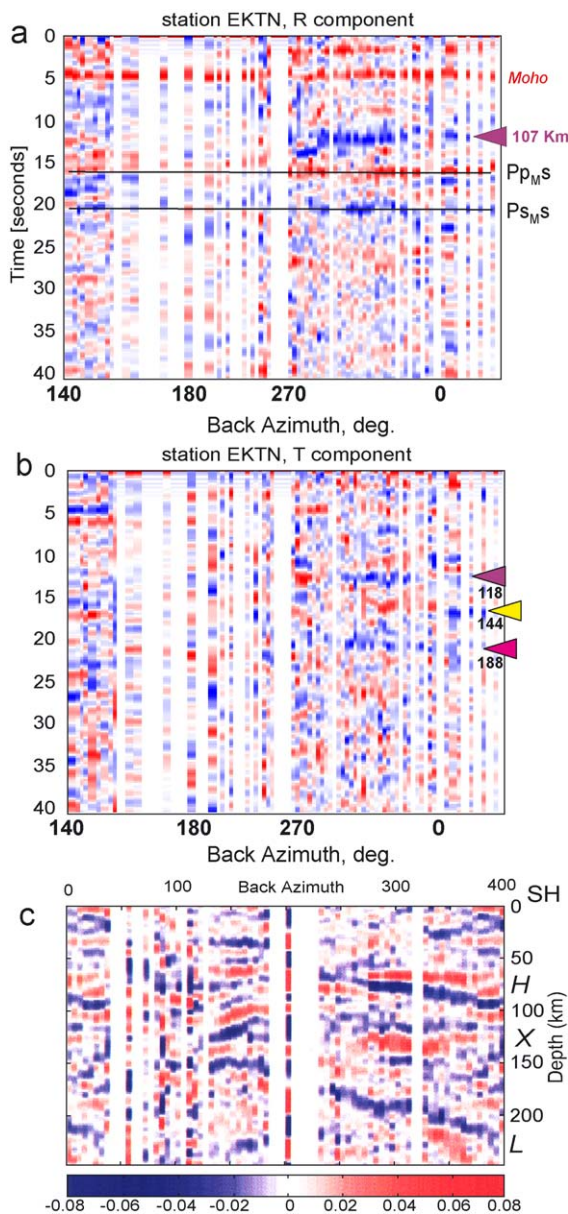
Fig. 3. Samples of summed impulse response or ‘receiver functions’ for POLARIS stations COWN, EKTN and MGTN (see Fig. 1). Each station has a pair of traces mapped to depth: the top is for radial (R) wave motion, the bottom for transverse (T) motion. Large triangles and associated numbers indicate depths to major discontinuities; small triangles mark reverberations (multiples) from the Moho discontinuity. Note that only the EKTN station has a strong signal on both functions at about 110 km. The receiver functions shown for these three stations used 94, 245 and 94 earthquake sources, respectively.

Other prominent discontinuities at 110–120 and 140–150 km depths observed on the transverse components at multiple stations indicate that a layer of low velocity or distinct anisotropy exists between these depths (Fig. 3). The coherency of pulses at about 13 s on the radial component indicates a strong decrease in velocity at 107 km depth north and west of Ekati, but

no such feature to the south (Fig. 4a). Similarly, the response on the transverse component for station EKTN indicates a change in anisotropic fabric at 118 km depth, a different one at 144 km, and another at 188 km. A flip in polarity at a back azimuth of about 280° occurs in the 118 km discontinuity and marks an axis of symmetry of anisotropy, here prob-

ably the dip direction of steep layering or planar fabric.

In the SW Slave craton north of Yellowknife similar discontinuities were observed on the transverse component at nominal depths of 75, 135 and 180–220 km (Fig. 4c, Bostock, 1998). The shallowest of these is the most clearly defined and comprises a sharp-topped layer 10 km thick that exhibits 5% S-wave anisotropy with a polarity flip at about 260°



back azimuth. A number of weak discontinuities at 8, 12 and 20 s can also be recognized beneath the central Kaapvaal craton using the same analytical technique and data from a local, temporary array near Kimberley (Fig. 5; James et al., 2001; but see Gao et al., 2002).

4. Layered anisotropy

A second method, applied to data from independent stations, estimates regional-scale fabric or layering within the mantle using differential travel times of S-waves caused by seismic anisotropy. The anisotropy typically arises from preferred fabric orientations; cracks are an obvious example in near-surface environments. Alignment of minerals such as olivine over large volumes and macroscopic layering of peridotite and eclogite are other possible causes of mantle anisotropy. Seismic waves that originate as S-waves, but travel through the Earth's molten core as P-waves before converting back to S-waves, so-called SKS and SKKS phases, are particularly suitable for anisotropy studies of the mantle beneath the receiver (Silver, 1996; Savage, 1999 are useful reviews). Within the mantle, olivine is the primary anisotropic mineral and fast polarization aligns parallel to the mineral *a*-axes. Peridotitic xenolith samples from the Kaapvaal exhibit up to 8% anisotropy for P-waves and 6% for S-waves (Ben-Ismaïl et al., 2001). In general, olivine *a*-axes concentrate within the foliation plane and parallel to lineations, whatever the cause of the foliation. It thus appears that S-wave energy propagating and vibrating within the plane of a vertical fabric travels faster than does energy vibrating perpendicular to the fabric; the

Fig. 4. Radial (a) and transverse (b) impulse responses as a function of back azimuth (incomplete suite of 1° bins) at the Ekati Diamond Mine™ station (EKTN on Fig. 1). Amplitudes are normalized to that of the incident P-wave, red is positive polarity, blue negative. Coverage is incomplete after 3 years of data collection; a back azimuth of 0 is North. The flat, consistent Moho response results in several multiples (PpMs and PsMs, see Fig. 2) at greater delay times. Only phases marked by arrowheads are considered probable mantle discontinuities at the depths indicated. Note the change of polarity at about 280° on the transverse component at these depths; a feature expected from anisotropy. (c) Transverse (SH) impulse response mapped to depth as a function of back azimuth (5° bins) at the Yellowknife array (modified from Bostock, 1998). The absence of significant Moho response on this component affords a window into the mantle where the H, X and L discontinuities are clearly visible.

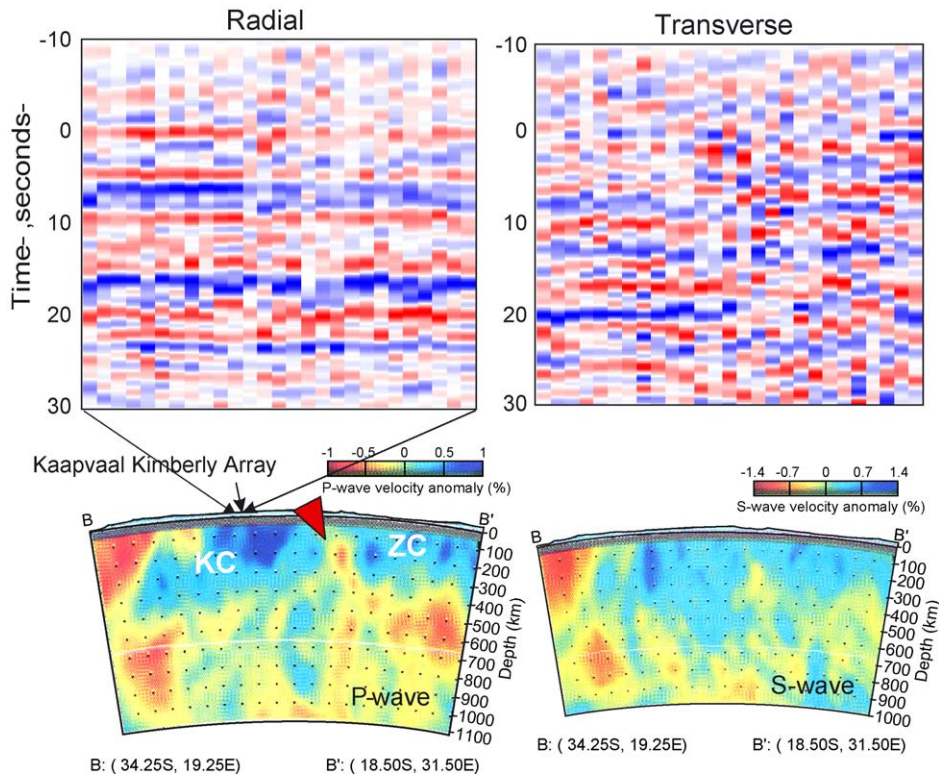


Fig. 5. (Top) Radial and transverse impulse responses as a function of back azimuth at the Kimberley broadband array (James et al., 2001). This is an east–west cross section through the array with each station projected perpendicularly onto the section. (Bottom) Tomographic cross sections for P-wave velocities (left) and S-wave velocities (right) of the Kaapvaal (KC) and Zimbabwe (ZC) cratons using data and methods as in Fig. 9; image from James et al. (2001).

difference in time of arrival is called the delay time, dt . The analysis also reveals the direction of the fast propagation axis, Φ (Fig. 6; online Appendix A). Typically, months of data are analyzed in order to produce an average anisotropy measurement for an assumed single layer of uniform anisotropy beneath each station, but observations made over two or more years often provide much additional and valuable information. Only two teleseismic stations in the NWT (Yellowknife and EKTN) have to date recorded a sufficient number of earthquakes appropriate for SKS analysis to reveal reliable trends.

The variations in the arrival of SKS phases with earthquake back azimuth (direction at which seismic wave arrives) reveal patterns (Fig. 6) that can be modeled by multiple or dipping layers of anisotropy (Vinnik et al., 1992; Rumpker and Silver, 1998; Levin and Park, 1998; Savage, 1999). The observed azi-

muthal variation at station EKTN within the central Slave cannot represent a single uniform layer because systematic variation with back azimuth exceeds uncertainties associated with the measurements. The observed variations can be most simply modeled by assuming two distinct horizontal layers within the lithosphere, each with a horizontal axis of hexagonal anisotropy symmetry. The back azimuths at which minimum delay times and very large delay times occur are particularly diagnostic in such two-layer models. The minimum marks the fast axis of anisotropy in the dominant layer, the associated delay time is that of the secondary anisotropy layer. The large delays mark interference between the two anisotropic layers where individual analyses produce nulls, unstable or large uncertainties. The analysis for EKTN reveals a shallow layer with about a third of the total observed anisotropy and a fast axis oriented at 006° ; a

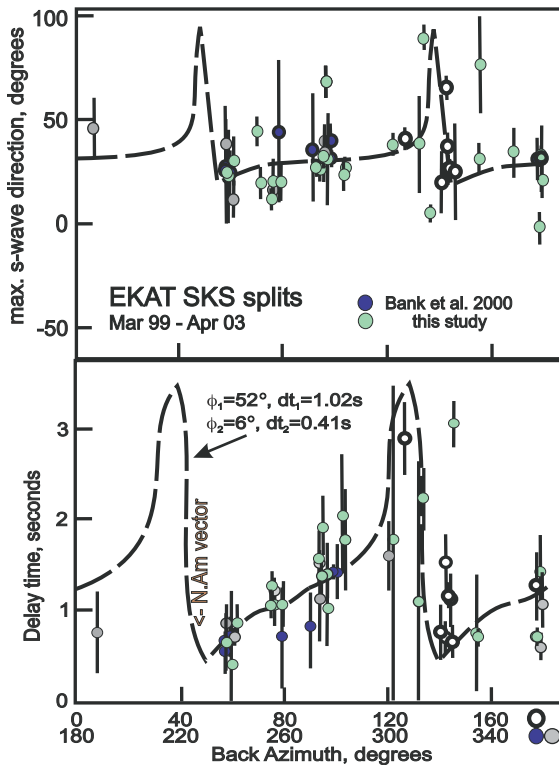


Fig. 6. Plots of the apparent fast polarization direction (top) and delay or splitting time (bottom) as a function of back azimuth for station EKAT (now POLARIS station EKTN) assuming a frequency of 0.08 Hz. Splitting parameters repeat every 180° so that the observations from both hemispheres are superimposed; open circles are observations from 0° to 180° , solid circles from 181° to 360° . The observations have standard uncertainties (e.g. Silver, 1996) shown by vertical bars. Grey dots are measurements at stations EKAT, EKTN, and NORMS. The wide, dashed line shows the predicted variation of these parameters for a two-layer model (Silver and Savage, 1994) with the parameters indicated in the lower graph. The predictive model repeats every 90° so that the observational gap from 0° to 60° is not debilitating.

deeper layer with the remainder of the anisotropy has a fast direction of 052° that coincides with present-day North American plate motion (Bank et al., 2000).

5. Layer interpretation

Together, the two independent, single-station techniques reveal two layers of anisotropy, three mantle discontinuities, and the Moho beneath the Ekati Diamond Mine™ site. The lower anisotropy layer prob-

ably lies deeper than 150 km in the mantle because the anisotropy aligns with both North American plate motion and the $\sim N50^\circ E$ strike of deep mantle structures identified previously by mantle geochemical analyses. The near-coincidence of the slow direction (276°) in the upper anisotropy layer and the polarity flip observed in the 118-km discontinuity suggest a common cause: that the discontinuity marks the top or bottom of the upper anisotropic layer.

The upper layer and 118-km discontinuity coincide with a prominent regional conductor identified by magnetotelluric studies (Jones et al., 2001), as well as with an ultra-depleted harzburgite layer identified from studies of garnets extracted from xenoliths in kimberlite core (Fig. 7) (Griffin et al., 1999; Kopylova and Russell, 2000). Ultra-depleted harzburgite is nearly pure olivine in composition and has potential for high anisotropy if individual olivine crystals are aligned (e.g. Silver, 1996). It appears probable that beneath station EKTN the upper anisotropic layer lies between 118 and 140 km, is anomalously conductive, and is composed of ultra-depleted harzburgite. The 190-km discontinuity may similarly mark the top of the deeper anisotropy layer. However, anisotropy within the crust, above 110 km, and at 140–190 km depths cannot be excluded.

The 110- and 140-km seismic discontinuities observed beneath the central Slave are not typical of cratons globally (Fig. 8). The ‘Hales’ discontinuity (Hales, 1969) is commonly associated with the spinel to garnet phase change found at 60–80 km depths and the ‘Lehman’ discontinuity (Lehman, 1955) appears beneath continents at ~ 220 km depth (Bostock, 1999, and references therein). The latter has been hypothesized as the base of an anisotropic layer below which aligned textures in peridotite are annealed and thus made more random and isotropic; it may represent the base of the lithosphere (Jordan, 1988). Thybo and Perchuc (1997) proposed that a layer of lower velocity and anisotropy due to partial melt at 100–150 km depths underlies a generally stratified uppermost mantle.

Because of the poor correlation among global seismic discontinuities, all three discontinuities observed beneath the Yellowknife area were instead interpreted as underthrust or underplated blocks of Archean crust or mantle, and linked to mantle reflectors observed on the LITHOPROBE SNORCLE line

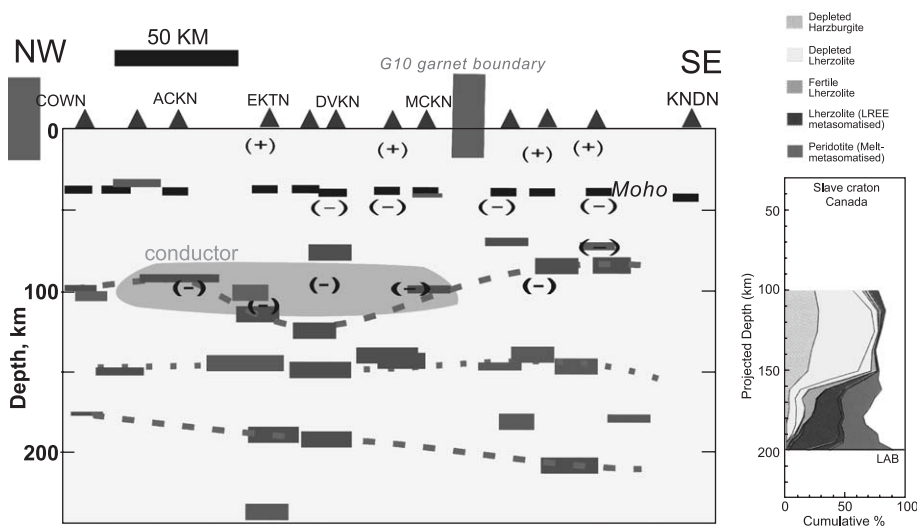


Fig. 7. Discontinuities beneath the central Slave craton. Seismic stations labeled are located at: Kennady Lake (KNDN), NE McKay Lake (MCKN), the Diavik mine airstrip (DVKN), the Ekati mine airstrip (EKTN), Achilles Lake (ACKN) and SW of Contwoyto Lake (COWN). Pluses and minuses represent discontinuities with changes in velocity identified from radial components. Bars represent discontinuities identified beneath individual stations on the transverse component. Smaller bars indicate less reliable estimates. Petrologic column from Griffin et al. (1999); conductor from Jones et al. (2001).

1 seismic reflection profile (Bostock, 1998). A pair of Proterozoic (1.89 – 1.84 Ga) subduction zones is the current preferred interpretation of these mantle reflectors (Cook et al., 1999). It is interesting to speculate that one or both of these Proterozoic underthrust or

subducted layers may continue NW of Yellowknife and into the central Slave near station EKTN. The surface expression of these convergence structures is the Wopmay orogen along the western margin of the Slave craton (Fig. 1). In order to correlate the mantle

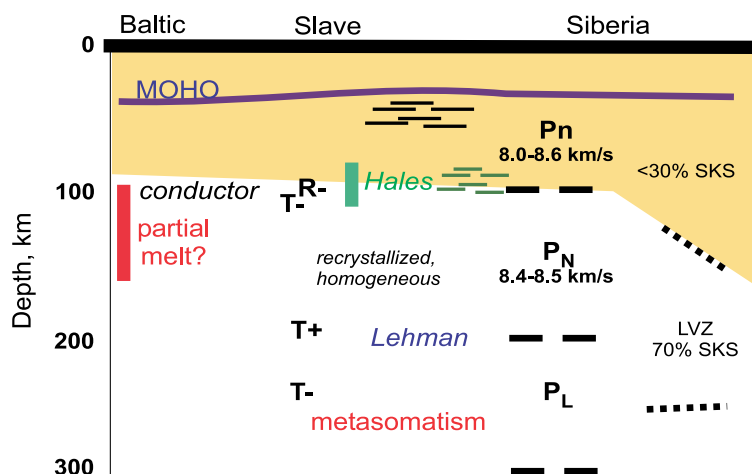


Fig. 8. Cartoon summary of upper mantle discontinuities observed globally beneath cratons and major continental blocks. Siberia structures are based on results from ‘peaceful’ nuclear explosion surveys (Pavlenkova, 1997; Oreshin et al., 2002). Baltic structures were described by Thybo and Perchuc (1997) and Kovtun and Porokhava (1980). Slave structure as described here and by Bostock (1998, 1999). Groups of short horizontal segments represents 1–2-km-thick layering inferred from scattering of seismic waves to the surface (Tittgemeyer et al., 1996).

discontinuities beneath Yellowknife and EKTN, one must invoke a complex subduction zone geometry with steeply (30°) and flat-dipping segments as is currently observed beneath the Andes of South America (Isacks, 1988). Alternatively, crustal stratigraphic studies suggest that the central Slave may be underlain by an older (2.6 Ga) convergent zone or suture (Bleeker et al., 1999).

6. Tomography, surface wave and scattering studies using arrays

Three other seismic analysis techniques with promising application to the mantle structure studies described here are currently in use elsewhere worldwide, but have only produced preliminary results for the Slave craton due to the lack of a suitable array of stations. One widely used tomography method inverts observed travel times of seismic P-wave arrivals using a large number of rays connecting earthquake–station pairs in order to estimate bulk, average velocities in a 3-D mantle volume (Van Decar, 1991). Because most of these seismic waves travel nearly vertically through the mantle, lateral resolution is generally good whereas vertical resolution is poor.

Within the Slave craton, this method was originally used in a reconnaissance analysis of the entire craton using 14 seismic stations (Fig. 1) that recorded 226 earthquakes (Bank et al., 2000). This data set was enhanced using the newly installed POLARIS array stations that had recorded an additional 120 earthquakes, thus adding 1149 new rays to the 1575 used previously. The new analysis removed all travel-time residuals <0.2 s and included 10 independent trials at reducing travel-time residuals, in which each trial involved 10,000 iterations. The resulting P-wave tomographic slowness ($1/\text{velocity}$) model has more detail in the central Slave area (Fig. 9) than did the reconnaissance survey, but retains all the major regional trends and features such as slower velocities beneath the Proterozoic terranes to the west (Bank et al., 2000). Depth slices at 170 and 230 km depths show a major transition parallel to and nearly coincident with the northern garnet geochemical boundary as defined by Grütter et al. (1999). POLARIS stations south of their southern garnet geochemical boundary

are underlain by slower velocity mantle than those to the north.

The strong lateral velocity variations shown on a north–south cross section through the tomography model (Fig. 9) suggest that the mantle discontinuities discussed previously do not represent laterally continuous layers, but rather the tops and bottoms of irregular blobs. The lack of well-defined layering is partly attributable to the poor depth resolution in the tomography model, but also suggests a relatively fine-scale structure within the mantle of the central Slave craton. The two analytical results do show consistent features in many places. For example, discontinuities at 80–110 km depths with an associated decrease in velocity with depth correlate well with the velocity model.

Similar tomographic analysis applied to the Kaapvaal and Zimbabwe cratons in southern Africa showed a high-velocity tectospheric keel to 250 km depth and, between the cratons, lower velocities within a zone dipping northeast beneath the Bushveld province (Fig. 5) (James et al., 2001). Velocity variation within the uppermost 200–300 km of the cratons is less pronounced here than in the central Slave craton, but diamond parageneses do generally correlate with bulk mantle velocity variations beneath southern Africa (Shirey et al., 2002). Diamonds from kimberlites erupted through seismically fast lithosphere are dominantly mid-Archean and peridotitic whereas those from slower lithosphere are mostly Proterozoic and eclogitic.

A second seismic method attempts the inversion of surface waveforms (Forsyth and Li, *in press*). It relies on interference of two incoming waves and depends on laterally and azimuthally varying phase velocities measured between two or more stations. The method recovers 2-D phase velocity maps for a series of narrow frequency bands that match specific depth ranges; longer period waves sample at greater depth. This method can therefore help constrain the location of anisotropy in the mantle, and estimate lithospheric thickness. As in tomography, resolution depends on the density of obliquely intersecting rays over the study area and the trade-off between model roughness and assumed anisotropy. Based on previous results elsewhere (Weeraratne et al., 2003), surface-wave inversion of the Slave array data should resolve anomalies with lateral wavelengths >100 – 150 km. Results will also be utilized in conjunction with SKS-

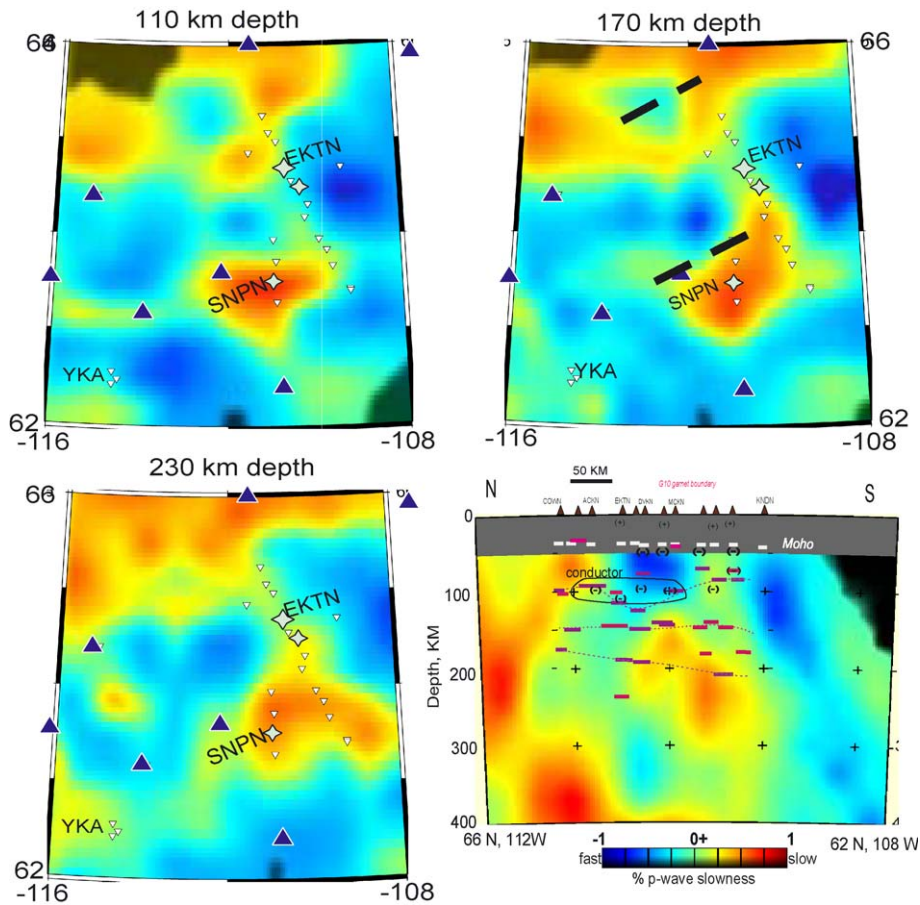


Fig. 9. Tomography-derived 3-D velocity models of the Slave craton; shown are depth slices at 110, 170 and 230 km and a north–south cross section. Modeling used the method and stations (black triangles) used by Bank et al. (2000) supplemented by POLARIS stations (white stars and inverted triangles). Black areas occur where fewer than four rays crossed the model cell. Black dash lines show geochemical boundaries (Grütter et al., 1999). See Fig. 7 caption for annotations on the cross section.

splitting analysis to constrain better the depth of anisotropic layers within the mantle.

A third analysis technique using seismic array data has not been attempted in the central Slave, but is planned once the array has sufficient length and density. Results from its recent application to the Cascadia subduction zone (Rondenay et al., 2001; Bostock et al., 2002) are shown (Fig. 10) here to demonstrate the potential for resolving similar, distinct mantle layers beneath cratons. Multiparameter two-dimensional inversion of scattered teleseismic waves repositions seismic energy arriving after the main P-wave to the depth where it was converted or scattered at major structures or seismic discontinuities

(Bostock et al., 2001). The clear imaging of two different Moho discontinuities as well as subducting oceanic crust beneath Cascadia approaches that achieved with deep seismic reflection profiling techniques and indicates that similar results should be possible where strong mantle discontinuities are already identified, such as in the central Slave craton.

7. Emerging technology drives new models of mantle structure

As was the case in southern Africa, the seismic results aid us in constructing a three-dimensional

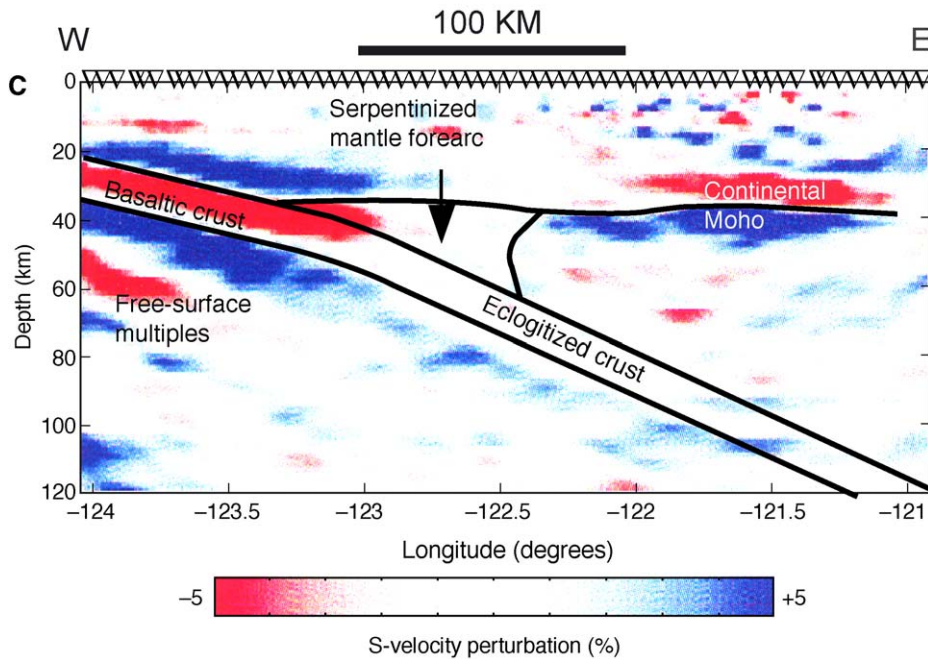


Fig. 10. S-wave velocity perturbations below a dense seismic array across the Cascades of central Oregon, USA (from Rondenay et al., 2001). Scattered waves in the P-wave coda of 31 earthquakes recorded at teleseismic distances were recovered from simultaneous inversion of signal recorded at 69 sites. This is a bandpass-filtered version of the true perturbations to a one-dimensional, smoothly varying reference model; discontinuities are present where steep changes (e.g. red to blue) in polarity occur.

model of the Slave craton from the surface to 700 km depths that is tied to surface geology and other geophysical and petrological constraints on mantle composition. It appears significant that major seismic discontinuities have associated changes in anisotropy more often than with increases or decreases in velocity or density with depth. The change in anisotropy at 118 km depth correlates with high conductivity that has been related to increased graphite content or connectivity (Jones et al., 2001). The change in anisotropy at 140 km depth correlates with an increase of metasomatism in mantle xenoliths (Fig. 7). It is not clear at present if these discontinuities represent the (dis)appearance of seismic anisotropy or just systematic re-orientations of anisotropic mantle structures. It is the combined use of seismic methods as described here that promises new understanding from powerful constraints on mantle structure, constraints not used in previous interpretations of mantle structure to our knowledge (Oreshin et al., 2002).

The preliminary tomography velocity models provide important three-dimensional information to the

discontinuity and anisotropy studies in that this method affords moderate and continuous horizontal resolution and lacks vertical resolution which the other methods provide. Early results suggest that the mantle geochemical trends implied from xenolith studies are not laterally continuous or relevant over large areas. For example, regions with slower velocities on the 170 and 230 km depth slices (Fig. 9) indicate that the southeastern-most source region for high-Cr G10 garnets is limited in extent and covers a triangular area of about 5000 km² that includes the Diavik, Snap Lake and Kennady Lake sites.

More precise definition of layers with properties such as increased carbon content or metasomatism has direct relevance to mapping potential source regions and long-term mantle reservoirs of diamonds. Once a mantle 'stratigraphy' is established and understood in terms of its seismic and other characteristics, its lateral extent can be mapped and related to broad changes in velocity. If the mantle layers derive from large-scale tectonic events, the resulting improved understanding of a region's geological history from surface mapping

and related geochemical and geochronological studies will also guide exploration models and strategies.

Continuing recording of earthquakes at the current 22 POLARIS stations and the infilling of the current array with additional stations will enable techniques such as travel-time tomography and inversions of scattered wavefields to provide more continuous 2-D and 3-D images of the lithosphere beneath the central Slave craton. Commonly observed discontinuities at 410- and 670-km depths appear sensitive to the thermal state of the mantle and may thus provide clues to the more recent kimberlite eruption processes. These various new results from the central Slave craton can also be compared and contrasted with similar studies and their recently published results from the Kaapvaal, Siberia and western Australia (Kennett et al., 1994; Debayle and Kennett, 2000; James et al., 2001; Oreshin et al., 2002; Simon et al., 2002). Meanwhile, we plan to install additional teleseismic stations during the next few years within other major cratons of North America.

Acknowledgements

The work presented here benefited from help from numerous sources, among them: members of the POLARIS consortium, especially Isa Asudeh, Calvin Andrews, Mike Patten and Gerrit Jansen van Beek for their efforts in installing field stations; Carolyn Relf, Hendrik Falck and John Armstrong of the CS Lord Geoscience Centre (Yellowknife, NWT); the staff of the Yellowknife Seismic Observatory; Wouter Bleeker, Bill Davis, Herman Grütter, and Alan Jones for many interesting discussions. This work was funded under Letters of Agreement between the Geological Survey of Canada, BHP-Billiton Diamonds; DeBeers Canada; and Kennecott Canada Exploration. POLARIS equipment was purchased through a Canadian Foundation for Innovation grant to Carleton University. Geological Survey of Canada contribution 2003060.

References

- Bank, C.-G., Bostock, M.G., Ellis, R.M., Cassidy, J.F., 2000. A reconnaissance teleseismic study of the upper mantle and transition zone beneath the Archean Slave craton in NW Canada. *Tectonophysics* 319, 151–166.
- Ben-Ismaïl, G., Barroul, R., Mainprice, D., 2001. The Kaapvaal seismic anisotropy: petrophysical analysis of upper mantle kimberlite nodules. *Geophysical Research Letters* 28, 2497–2500.
- Bleeker, W.J., Ketchum, W.F., Jackson, V.A., Villeneuve, M., 1999. The central slave basement complex. Part I: its structural topology and autochthonous cover. *Canadian Journal of Earth Sciences* 36, 1083–1109.
- Bostock, M.G., 1998. Seismic stratigraphy and evolution of the Slave province. *Journal of Geophysical Research* 103, 21183–21200.
- Bostock, M.G., 1999. Seismic imaging of lithospheric discontinuities and continental evolution. *Lithos* 48, 1–16.
- Bostock, M.G., Rondenay, S., Shragge, J., 2001. Multiparameter two-dimensional inversion of scattered teleseismic body waves. 1: theory for oblique incidence. *Journal of Geophysical Research* 106, 30771–30794.
- Bostock, M.G., Hyndman, R.D., Rondenay, S., Peacock, S.M., 2002. An inverted continental Moho and serpentinization of the forearc mantle. *Nature* 417, 536–538.
- Cook, F.A., van der Velden, A., Hall, K.W., Roberts, B.J., 1999. Frozen subduction in Canada's Northwest Territories: LITHOPROBE deep lithospheric reflection profiling of the western Canadian Shield. *Tectonics* 18, 1–24.
- Davis, W.J., Gariépy, C., van Breeman, O., 1996. Pb isotopic composition of Late Archean granites and the extent of recycling early Archean crust in the Slave Province, northwest Canada. *Chemical Geology* 130, 255–269.
- Debayle, E., Kennett, B.L.N., 2000. Anisotropy in the Australian upper mantle from Love and Rayleigh waveform inversion. *Earth and Planetary Science Letters* 184, 339–351.
- Forsyth, D.W., Li, A., 2003. Array-analysis of two-dimensional variations in surface wave velocity and azimuthal anisotropy in the presence of multipathing interference. In: Levander, A., Nolet, G. *Seismic Data Analysis and Imaging with Global and Local Arrays*. American Geophysical Union Geophysical Monograph. in press.
- Gao, S.S., Silver, P.G., Liu, K.H., the Kaapvaal Seismic Group, 2002. Mantle discontinuities beneath Southern Africa. *Geophysical Research Letters* 29, 10 (DOI 10.1029/2001GL013834).
- Griffin, W.L., Doyle, B.J., Ryan, C.G., Pearson, N.J., O'Reilly, S.Y., Davies, R.M., Kivi, K., van Achterbergh, E., Natapov, L.M., 1999. Layered mantle lithosphere in the Lac de Gras area, Slave Craton: composition, structure, and origin. *Journal of Petrology* 40, 705–727.
- Grütter, H.S., Apter, D.B., Kong, J., 1999. Crust–mantle coupling: evidence from mantle-derived xenocrystic garnets. In: Gurney, J.J., Richardson, S.R. (Eds.). *Proc. 7th Kimberlite Conference, Red Roof Design, Cape Town*, 307–312.
- Hales, A.L., 1969. A seismic discontinuity in the lithosphere. *Earth and Planetary Science Letters* 7, 44–46.
- Isacks, B.L., 1988. Uplift of the central Andean plateau and bending of the Bolivian orocline. *Journal of Geophysical Research* 93, 3211–3231.
- James, D.E., Fouch, M.J., VanDecar, J.C., van der Lee, S., Kaapvaal Seismic Group, 2001. Tectosphere structure beneath southern Africa. *Geophysical Research Letters* 28, 2485–2488.

- Jones, A.G., Ferguson, I.J., Chave, A.D., Evans, R.L., McNeice, G.W., 2001. Electric lithosphere of the Slave craton. *Geology* 29, 423–426.
- Jordan, T.H., 1988. Structure and formation of the continental tectosphere. *Journal of Petrology*, 11–37 (Special Lithosphere Issue).
- Kennett, B.L.N., Gudmunsson, O., Tong, C., 1994. The upper mantle S and P velocity structure beneath northern Australia from broadband observations. *Physics of the Earth and Planetary Interiors* 86, 85–98.
- Kopylova, M.G., Russell, J.K., 2000. Chemical stratification of cratonic lithosphere: constraints from the northern Slave craton, Canada. *Earth and Planetary Science Letters* 181, 71–87.
- Kovtun, A.A., Porokhava, L.N., 1980. Deep conductivity distribution of the Russian platform from the results of combined magnetotelluric and global magnetovariational data interpretation. *Journal and Geomagnetism and Geoelectricity* 32 (Suppl. 1), 105–133.
- Lehman, I., 1955. The times of P and S in northeastern America. *Annales Geofisica* 8, 351–370.
- Levin, V., Park, J., 1998. P–SH conversions in layered media with hexagonal symmetric anisotropy: a cookbook. *Pure and Applied Geophysics* 151, 669–697.
- Nolet, G., Grand, S.P., Kennett, B.L.N., 1994. Seismic heterogeneity in the upper mantle. *Journal of Geophysical Research* 99, 23753–23766.
- Oreshin, S., Vinnik, L., Makeyeva, L., Kosarev, G., Kind, R., Wentzel, F., 2002. Combined analysis of SKS splitting and regional P traveltimes in Siberia. *Geophysical Journal International* 151, 393–402.
- Pavlenkova, N.I., 1997. General features of the upper mantle structure from seismic data. In: Fuchs, K. (Ed.). *Upper Mantle Heterogeneities from Active and Passive Seismology*. Kluwer Academic Publishing, Netherlands, pp. 225–236.
- Rondenay, S., Bostock, M.G., Shragge, J., 2001. Multiparameter two-dimensional inversion of scattered teleseismic body waves. 3: application to the Cascadia 1993 data set. *Journal of Geophysical Research* 106, 30795–30807.
- Rümpker, G., Silver, P.G., 1998. Apparent shear-wave splitting parameters in the presence of vertically varying anisotropy. *Geophysical Journal International* 135, 790–800.
- Savage, M.K., 1999. Seismic anisotropy and mantle deformation: what have we learned from shear wave splitting. *Review of Geophysics* 37, 65–106.
- Shirey, S.B., Harris, J.W., Richardson, S.H., Fouch, M.J., James, D.E., Cartigny, P., Deines, P., Viljoen, F., 2002. Diamond genesis, seismic structure, and evolution of the Kaapvaal–Zimbabwe craton. *Science* 297, 1683–1686.
- Silver, P.G., 1996. Seismic anisotropy beneath the continents: probing the depths of geology. *Annual Review of Earth and Planetary Sciences* 24, 385–432.
- Silver, P.G., Savage, M.K., 1994. The interpretation of shear wave splitting parameters in the presence of two anisotropic layers. *Geophysical Journal International* 119, 949–963.
- Simon, R.E., Wright, C., Kgaswane, E.M., Kwadiba, M.T.O., 2002. The P wavespeed structure below and around the Kaapvaal craton to depths of 800 km, from traveltimes and waveforms of local and regional earthquakes and mining-induced tremors. *Geophysical Journal International* 151, 132–145.
- Snyder, D.B., Asudeh, I., Darbyshire, F., Drysdale, J., 2002. Field-based feasibility study of teleseismic surveys at high northern latitudes, Northwest Territories and Nunavut. *Current Research - Geological Survey of Canada* 2002-C3 (10 pp.).
- Thybo, H., Perchuc, E., 1997. The seismic 8° discontinuity and partial melting in continental mantle. *Science* 275, 1626–1629.
- Tittgemeyer, M., Wenzel, F., Fuchs, K., Ryberg, T., 1996. Wave propagation in a multiple-scattering upper mantle—observations and modeling. *Geophysical Journal International* 127, 492–502.
- Van Decar, J.C., 1991. Upper-mantle structure of the Cascadia subduction zone from non-linear teleseismic travel-time inversion. PhD thesis, University of Washington, Seattle, WA.
- Vinnik, L.P., Makayeva, L.I., Milev, A., Usenko, A.Y., 1992. Global patterns of azimuthal anisotropy and deformations in the continental mantle. *Geophysical Journal International* 111, 433–447.
- Weeraratne, D.S., Forsyth, D.W., Fischer, K.M., Nyblade, A.A., 2003. Rayleigh wave tomography evidence for an upper mantle plume beneath the Tanzanian craton. *Journal of Geophysical Research* 108 (B9), 2427.